



UNESCO Chair on
Coastal Geo-Hazard Analysis



Research Institute for Earth Sciences
Geological Survey of Iran

Chair



UNESCO Chair on
Coastal Geo-Hazard Analysis



Research Institute for Earth Sciences
Geological Survey of Iran

Chair

Abstract:

The main goal of this study is ground magnetic survey, induced polarization and resistivity methods, in order to detect the Astara Fault trace. In this regard 4 data acquisition was undertaken at 4 different areas, namely: Gisum, Lisar, Talesh and Jokandan.

Generally, in sedimentary basins faults are accompanied with a linear anomaly in magnetic field data. Even layers with weak magnetization, can show a magnetic linear structure along faults. For this reason, any magnetic methods are a good tool for detecting faults without any clear morphological evidences on the ground. There are some methods such as horizontal and vertical derivatives and reduce of the magnetic pole, to support the shape and geometry of faults.



Geophysical Investigation along the Astara Fault; Geomagnetic and Goelectric methods

ISBN: 978-622-5858-69-5

2023



9 786225 858695

UCCGHA 015

2023

Geophysical Investigation along the Astara Fault; Geomagnetic and Geoelectric methods



- سرشناسه : اسعدی، واحد، ۱۳۶۹-
-Asadi, Vahed, 1990
- عنوان و نام پدیدآور : Geophysical investigation along the Astara fault; geomagnetic and geoelectric methods [Book]/ author Vahed Asadi, Farhad Sobouti, Mahnaz Rezaeian; employer University of Basic Sciences, Zanjan; advisor Research Institute for Earth Sciences; supervisor Hamid Nazari; Summarized and translated into English Manouchehr Ghorashi; with cooperation UNESCO Chair on Coastal Geo-Hazard Analysis.
- مشخصات نشر : تهران: نشر خزه، ۱۴۰۲ = ۲۰۲۳ م.
- مشخصات ظاهری : ۷۴ ص.: مصور(رنگی)، جدول، نمودار؛ ۱۴/۵ × ۲۱/۵ س.م.
- شابک : 978-622-5858-69-5
- وضعیت فهرست نویسی : فیبا
- یادداشت : زبان: انگلیسی.
- یادداشت : عنوان به فارسی: شناسایی گسل فعال آستارا با استفاده از روش‌های ژئوالکتریک و ژئومغناطیس.
- یادداشت : کتابنامه: ص.۵۷.
- آوانویسی عنوان : جئوفیزیکال...
موضوع : گسله‌ها -- ایران -- آستارا
- موضوع : Faults, (Geology) -- Iran -- Astara
- شناسه افزوده : ثبوتی، فرهاد، ۱۳۴۴-
- شناسه افزوده : Sobouti, Farhad, 1965-
- شناسه افزوده : رضائیان، مهناز، ۱۳۶۱-
- شناسه افزوده : Rezaeian, Mahnaz, 1982-
- شناسه افزوده : قریشی، منوچهر، مترجم
- شناسه افزوده : Ghorashi, Manouchehr
- شناسه افزوده : نظری، حمید، ۱۳۴۶-، ناظر
- شناسه افزوده : یونسکو. کرسی مخاطرات زمین شناختی ساحلی
- شناسه افزوده : UNESCO Chair on Coastal Geo-Hazard Analysis
- شناسه افزوده : دانشگاه تحصیلات تکمیلی علوم پایه زنجان
- شناسه افزوده : University of Basic Sciences, Zanjan
- شناسه افزوده : سازمان زمین‌شناسی و اکتشافات معدنی کشور. پژوهشکده علوم زمین
- شناسه افزوده : Geological Survey & Mineral Exploration of Iran. Institute of Earth Sciences
- رده بندی کنگره : ۵/۲۰۴۱ ۹ج۵الف/QE۶۰۶
- رده بندی دیویی : ۷۸۲۰۹۵۵۳۲۶۶/۵۵۱
- شماره کتابشناسی ملی : ۹۴۱۳۱۹۸

Geophysical Investigation along the Astara Fault; Geomagnetic and Geoelectric methods

Author: Vahed Asadi





UNESCO Chair on
Coastal Geo-Hazard Analysis

Research Institute for Earth Sciences
Geological Survey of Iran



unesco
Chair



نشرخزه

اطلاعات گزارش

عنوان: شناسایی گسل فعال آستارا با استفاده از روش‌های ژئوالکتریک و ژئومغناطیس

مجری: دانشگاه تحصیلات تکمیلی علوم پایه گاوازنگ - زنجان

مشاور: پژوهشکده علوم زمین

زبان مرجع: فارسی

خروجی: گزارش، نقشه، مقاله، داده‌های الکترونیکی

ناظر علمی: حمید نظری

نویسندگان: واحد اسعدی، فرهاد ثبوتی، مهناز رضائیان

رئیس کرسی یونسکو در مخاطرات زمین‌شناختی ساحلی: حمید نظری

مسئول شورای اجرایی: راضیه لک

خلاصه‌نویسی و ترجمه به انگلیسی: منوچهر قرشی

خلاصه شده از: طرح مخاطرات زمین‌شناسی دریایی حوضه جنوب کاسپین

ناشر: نشر خزه

با همکاری کرسی یونسکو در مخاطرات زمین‌شناختی ساحلی

چاپ اول: ۱۴۰۲

شمارگان: ۵۰ نسخه

صفحات: ۷۴

شابک: ۹۷۸-۶۲۲-۵۸۵۸-۶۹-۵

khazepub@gmail.com



UNESCO Chair on
Coastal Geo-Hazard Analysis

Research Institute for Earth Sciences
Geological Survey of Iran



Report Information

Title: Geophysical Investigation along the Astara Fault;
Geomagnetic and Geoelectric methods

Employer: University of Basic Sciences, Zanjan

Advisor: Research Institute for Earth Sciences

Original language: Persian

Output: Report, Map, Paper, Digital Meta Data

Supervisor: Hamid Nazari

Authors: Vahed Asadi, Farhad Sobouti, Mahnaz Rezaeian

Chairholder in the UNESCO Chair on Coastal Geo-Hazard Analysis:
Hamid Nazari

Head of the Executive Council: Razyeh Lak

Summarized and translated into English: Manouchehr Ghorashi

Summarized after: Geohazard South Caspian Carpet (GSCC)

Publisher: Khazeh Publication

with cooperation UNESCO Chair on Coastal Geo-Hazard Analysis

First Edition: 2023

Edition number: 50

Page: 74

Shabak: 978-622-5858-69-5

khazepub@gmail.com

Scientific Council

Name	Affiliation
Ara Avagyan	IGS: Institute Geological Sciences
Rick J Bailey	IOC-UNESCO Indian Ocean Tsunami Warning and Mitigation System/ UNESCO
Aram Fathian Baneh	University of Calgary
Wenjiao Xiao	Chinese Academy of Sciences
Magdi Guirguis	Institut français d'archéologie orientale du Caire
Richard Walker	University of Oxford
Philippe Agard	University of Sorbonne
Justin Ahanhanzo	Intergovernmental Oceanographic Commission of UNESCO (IOC-UNESCO)
Alice Aurelie	UNESCO Water Sciences Division
Eric Barrier	University of Sorbonne
Jean-François Ritz	University of Montpellier
Martin Hanz	German under water archaeology association
Klaus Reicherter	Aachen University
Judith Thomalsky	German Archaeological Institute Tehran Branch
Hamid Alizadeh Lahijani	Iranian National Institute for Oceanography and Atmospheric Science
Abbas Banj Shafiei	Urmia University
Yahya Djamour	Shahid Beheshti University (SBU)
Hassan Fazeli Nashli	University of Tehran
Razyeh Lak	Research Institute for Earth Sciences
Mohammad Mokhtari	International Institute of Earthquake

	Engineering and Seismology
Hamid Nazari	Research Institute for Earth Sciences
Jafar Omrani	Geological Survey of Iran
Morteza Talebian	Research Institute for Earth Sciences
Mohammad Tatar	International Institute of Earthquake Engineering and Seismology
Mahdi Zare	International Institute of Earthquake Engineering and Seismology
Stefano Salvi	National Institute of Geophysics and Volcanology (INGV)
Ryo Anma	Tokushima University
Yeong Bae Seong	Korea University
John Lambert	Deltares, UNESCO
Issa El-Hussain	Sultan Qaboos University
Ekkehard Holzbecher	German University of Technology in Oman
Egor Krasinskiy	Underwater research center Russian Geographical Society
Audemard Franck A.	Department of Geology, Central University of Venezuela

Executive Committee

Name	Affiliation
Nasir Ahmadi	Environmental Protection Organization of Mazandaran Province
Arash Amini	Golestan University
Alireza Amrikazemi	Scientific Coordinator, Qeshm Island UNESCO Global Geopark
Parviz Armani	Imam Khomeini International University
Ataollah Dadashpour	Geological Survey of Iran, Sari branch

Asghar Dolati	Kharazmi University
Hasan Fazelinashli	University of Tehran
Abdolazaim Ghanghormeh	Golestan University
Habibolah Ghasemi	Shahrood University of Technology
Mohammad reza Ghasemi	Research Institute for Earth Sciences
Manouchehr Ghorashi	Research Institute for Earth Sciences
Jafar Hassanpour	University of Tehran
Ataollah Kavian	Environmental Protection Organization of Mazandaran Province
Mohammadreza Kazemzadeh	Superme Audit Gourt
Dr. Razyeh Lak	Head of RIES and Executive Manager
Mahmoudreza Majidifard	Research Institute for Earth Sciences
Ali Akbar Momeni	Shahrood University of Technology
Seyed Mohsen Mortazavi	Hormozgan University
Hasan Nasrollah Zadeh Saravi	Caspian Sea Ecological Research Center
Ehsan Pegah	Kharazmi University
Abdolwahed Pehpouri	Qeshm Island UNESCO Global Geopark
Ahmadreza Rabani	University of Science and Technology of Mazandaran
Mahdi Rahmanian	Shargh Daily newspaper
Ahmad Rashidi	International Institute of Earthquake Engineering and Seismology
Masoud Sadri Nasab	University of Tehran
Mohammad Salamati	Respina Company
Mohammad Tatar	International Institute of Earthquake Engineering and Seismology
Alireza Vaezi	Research Institute for Earth Sciences
Mojtaba Yamani	University of Tehran

Ahmed Hadidi	German University of Technology in Oman (GUTECH)
--------------	---

Secretariat

Name	Affiliation
Elnaz Aghaali	Research Institute for Earth Sciences
Keivan Ajdari	Research Institute for Earth Sciences
Hourieh AliBeygi	Research Institute for Earth Sciences
Sedigheh Ghanipour	Research Institute for Earth Sciences
Hamoon Memarian	Research Institute for Earth Sciences
Shirin Safavi	Research Institute for Earth Sciences
Aazam Takhtchin	Research Institute for Earth Sciences
Mehrnoosh Pour Saeid	Graphic Designer
Hanieh Bakhshaei	Geological Survey of Iran
Reza Behbahani	Geological Survey of Iran
Javad Darvishi khatooni	Geological Survey of Iran
Mohammadreza Ensani	Geological Survey of Iran
Marziyeh Estrabi Ashtiyani	Geological Survey of Iran
Gholamreza Hoseinyar	Geological Survey of Iran
Mojtaba Kavianpour Sangno	Geological Survey of Iran

Contents

1- Magnetic Fields Processing and Electric Acquisition for Determining Linear Trends and Ascertainment Depth of Magnetic Sources	1
1-1- Linear Magnetic Anomalies of Faults.....	1
1-2- Gisum Area, (First Stage).....	1
1-3- Gisum Area- Second Stage	5
1-3-1- Gridding Method.....	5
1-3-2- Total Magnetic Field Map	7
1-4- Using Filter For Recognition of Magnetic Anomalies	9
1-4-1- Conversion to Magnetic Pole.....	9
1-4-2- Vertical derivative.....	11
1-4-3- Horizontal Derivative.....	13
1-4-4- Analytical Signal.....	15
1-4-5- Upward Continuation.....	17
1-5- Gisum Area- Third Stage	19
1-6- Received Answers for Magnetic Source Depths with Euler Deconvolution Method.....	22
1-7- Resistivity Profiles and Induced Polarization	28
1-8- Lissar Area	40
1-9- Talesh area.....	44
1-10- Jokandan Area.....	48

2- Discussion and Conclusion.....	53
2-1- Lissar Area	53
2-2- Talesh Area	53
2-3- Jokandan Area.....	54
2-4- Gisum Area	54
2-4-1- Are Detected Linear Structures are Indication of Buried Faulting	55
References.....	57

Table of Figures

Figure 1: The data collection zone in Gisum region is marked in the red box. The place where the land falls and spring is marked with a white arrow. The cream-colored area on the mountainside represents a part of the survey area that was carried out on layers of limestone and calcareous sandstone, and a larger part on Quaternary alluvial sediments.....	3
Figure 2: The map of the total magnetic field intensity in the first phase of Gisum surveying is shown in this figure. The dashed line is the location of the high voltage power line. The collection stations are marked with red circles.	4
Figure 3: Comparison of two methods of least squares interpolation (right figure) and bidirectional method (left figure).....	6
Figure 4: Map of the total magnetic field. The surveying points are drawn with hollow circles. The small white square in the upper left corner is spring location. The three revealed linear trends are shown in the box.....	8
Figure 5: The map of converted magnetic anomaly pole.	10
Figure 6: Map of the vertical derivative of the magnetic field on converted magnetic pole. Magnetic linear trends can be observed clearly.	12
Figure 7: Map of the perfect horizontal derivative of the magnetic field converted to magnetic poles.....	14

Figure 8: Analytical signal map of magnetic field converted to magnetic pole. 16

Figure 9: Comparison of the map of conversion to the magnetic pole with the maps of continuing upwards at different altitudes. a) 10 meters. b) Upward continuation to 20 meters. c) 40 meters. d) 60 meters. n) 80 meters. f) 100 meters. e) 120 meters. j) 150 meters. As the height increases, high frequencies are attenuated and deeper anomalies are amplified. 19

Figure 10: Magnetic field anomaly map after removing the earth's magnetic field component. Surveyed points are marked with hollow circles. The direction of the lines is east-west and is drawn with black lines. 20

Figure 11: Comparison of magnetic field maps in two arrays in Gisum and location of magnetic linear trends. 21

Figure 12: A view of the geoelectric surveying site in Gisum region. View to the southwest. 29

Figure 13: Location of three geoelectric measurements on the magnetic field map and Google Earth satellite image. 30

Figure 14: A) The location of surveyed electric profile with the dipole-dipole array on the magnetic field map. b) Electrical resistance quasi-section. c) Chargeability quasi-section. The red arrows on the pseudo-sections indicate the location of the linear anomaly. 32

Figure 15: A) The location of measured electric profile with the dipole-dipole array on the magnetic field map. b) Electrical resistance quasi-section. c) Chargeability quasi-section. The area inside the dashed line is the

groundwater table. 1 and 2 show areas with lower resistance..... 33

Figure 16: A) The location of measured electric profile with the dipole-dipole array on the magnetic field map. b) Electrical resistance quasi-section. Corresponding to magnetic anomaly, electrical anomaly is observed. 1 and 2 show areas with higher resistance..... 34

Figure 17: A) The location of surveyed electric profile on the magnetic field map. b) Electrical resistance quasi-section. c) Chargeability quasi-section. Corresponding to the magnetic anomaly, the electrical anomaly is seen in the quasi-sections. The area inside the dashed line is the groundwater numbers. 1 and 2 show areas with lower resistivity..... 35

Figure 18: A) The location of surveyed electric profile on the magnetic field map. b) Electrical resistance quasi-section. 36

Figure 19: A) The location of surveyed electric profile by the polar-dipole method on the magnetic field map. b) Electrical resistance quasi-section. c) Chargeability quasi-section. Corresponding to the magnetic anomaly, the electrical anomaly is also observed. The area inside the dashed line is the groundwater table. 1 and 2 show areas with lower resistance and higher chargeability. .. 38

Figure 20: A) The location of surveyed electric profile with the reversed polar-dipole array on the magnetic field map. b) Electrical resistance quasi-section. Number 1 indicates the area with lower resistance..... 39

Figure 21: Geographical location of data collection site in Lisar area near Hareh Dasht village. The start and end

of the surveying points are marked with white arrows. The white line shows the navigation trend. 41

Figure 22: Anomalous profile of the magnetic field carried out along the river in Lisar. The location of the fault introduced by the Geological Survey of Iran is indicated by arrow number 2. The rest of the arrows show the location of the revealed abnormalities. 42

Figure 23: Geological map of the studied area. The surveying points are marked with a circle on the AB line. Q(t): alluvial sediments and alluvial fans. Ku(sl): sandy limestones of Upper Cretaceous age. Pe(vt): andesitic tuffs of Pliocene age. The reverse fault with strike-slip component is marked with a black line. 43

Figure 24: Bottom: Magnetic field anomaly map on Google Earth image. Measured lines in black. The designated fault is marked with a white line and the shutter ridge is marked with a red line. Q(t) Quaternary alluvial sediments and Pe(v.t) is andesitic tuffs. Figure above) Magnetic anomaly map. The black north-south line of the Astara fault has been determined by the Geological Survey of Iran. 47

Figure 25: The magnetic anomaly profile (TMA) in Talash is plotted with a red circle and the analytical signal (AS) with a black square. The arrow shows the location of the shutter ridge. 49

Figure 26: Above) Magnetic field anomaly map in Jokandan region. Surveying points are marked with circles on the map. The black lines numbered 1 to 4 are faults determined by the Geological Survey of Iran. The two yellow boxes are anomalies suspected to be caused

by faulting. (bottom figure) magnetic field map on the geological map of the area. Q(t): Quaternary alluvial deposits. Pe(v.t): Pliocene andesitic tuffs. Ku(sl): Upper Cretaceous sandy limestone..... 51

Figure 27: The profile of magnetic anomaly (red color) and analytical signal (black color) of AB in the river course of Jokandan region. The blue arrows are the locations of the faults determined by the Geological Survey of Iran. 52

1- Magnetic Fields Processing and Electric Acquisition for Determining Linear Trends and Ascertainment Depth of Magnetic Sources

The main goal of this study is ground magnetic survey, induced polarization and resistivity methods, in order to detect the Astara Fault trace. In this regards 4 data acquisition was undertaken at 4 different areas, namely: Gisum, Lisar, Talesh and Jokandan.

1-1- Linear Magnetic Anomalies of Faults

Generally, in sedimentary basins faults are accompanied with a linear anomaly in magnetic field data. Even layers with weak magnetization, can show a magnetic linear structure along faults. For this reason, any magnetic methods are a good tool for detecting faults without any clear morphological evidences on the ground. There are some methods such as horizontal and vertical derivatives and reduce of the magnetic pole, to support the shape and geometry of faults.

1-2- Gisum Area, (First Stage)

This site is located 10 km south of Asalem city (Figure 1). The traverse covers an area from the beach to the Talesh Mountain front. There is scarp with 2 m high, which probably is related to the fault movement. The trend of survey profiles is more or less E-W, perpendicular to the fault trace. Interval between survey points is 30 m, distance between lines is about 500 m,

and number of surveyed points are 1436 (Figure 2). Figure 2 shows the total magnetic intensity and surveying points. For gridding least square method used. As can be seen magnetic fields increase from west towards the east. This is because, in this area magnetic intensity is located in the negative pole of magnetic field of the Talesh Mountains. No sharp lineament in of total magnetic intensity can be seen in the map. In this reason, a smaller area selected for detail studies (Figure 2).

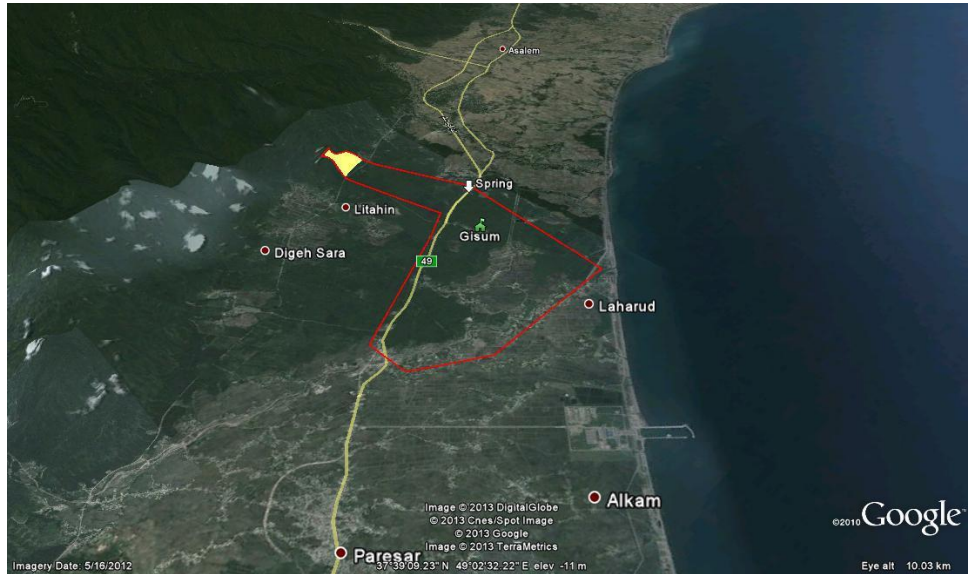


Figure 1: The data collection zone in Gisum region is marked in the red box. The place where the land falls and spring is marked with a white arrow. The cream-colored area on the mountainside represents a part of the survey area that was carried out on layers of limestone and calcareous sandstone, and a larger part on Quaternary alluvial sediments.

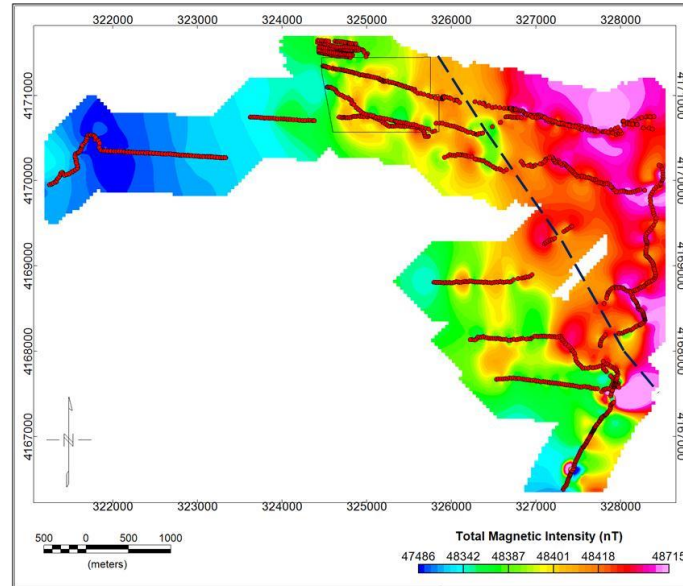


Figure 2: The map of the total magnetic field intensity in the first phase of Gisum surveying is shown in this figure. The dashed line is the location of the high voltage power line. The collection stations are marked with red circles.

1-3- Gisum Area- Second Stage

In this stage surveying is done in a smaller area (1300 m length and 300 m width). Distance between surveyed points of the lines are E-W and parallel. Total points are 1602, and survey lines are 23. It is worth to mention that the studied area in this locality covered completely by forest.

1-3-1- Gridding Method

For gridding the data which, obtained along the parallel lines, the bidirectional method can be used, but in compared between the least square and dimensional methods, better results can be obtained from the least square model. The reason is anomalies with smaller amplitude, and large distance between stations and surveyed lines. In Figure 3 the results of these methods are shown.

Geophysical Investigation along the Astara Fault; Geomagnetic and Geoelectric methods

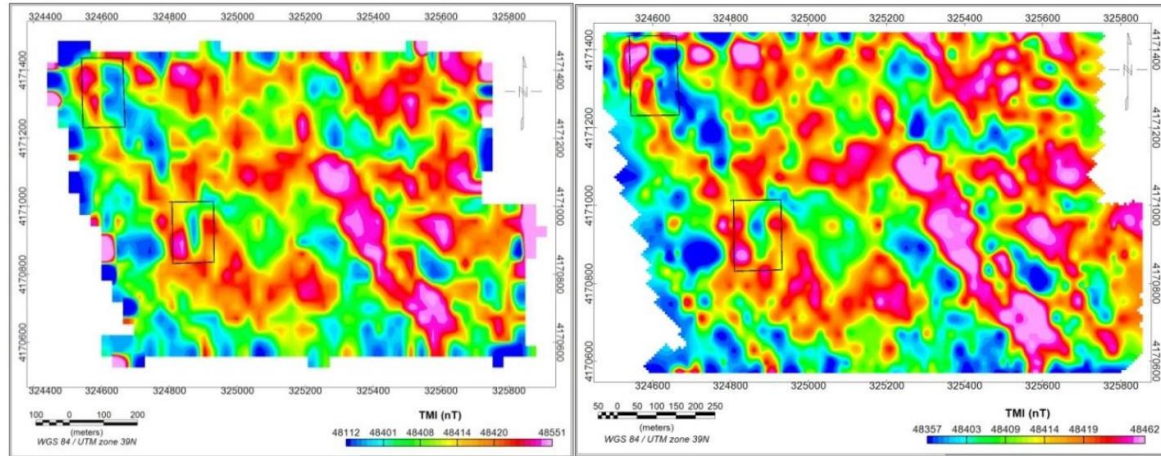


Figure 3: Comparison of two methods of least squares interpolation (right figure) and bidirectional method (left figure).

1-3-2- Total Magnetic Field Map

Figure 4, shows the total magnetic field map of the area. Dark blue color indicating minimum intensity field, and pink color showing the maximum intensity field. The maximum field is 42462 Nano tesla, minimum is 48381 Nano tesla, and average intensity is 48420 Nano tesla. There are three parallel magnetic anomaly lines with NW-SE trend numbered 1 to 3 in Figure 4. The amplitude of these anomalies are very low (about 40 Nano tesla), which is normal in sedimentary basins. Intervals between anomaly lines are about 100 m to 200 m. Greatest wave length and anomaly amplitude, is related to No.2 with about 100 m. The anomaly No.1, the same as 2 and 3 is not clear.

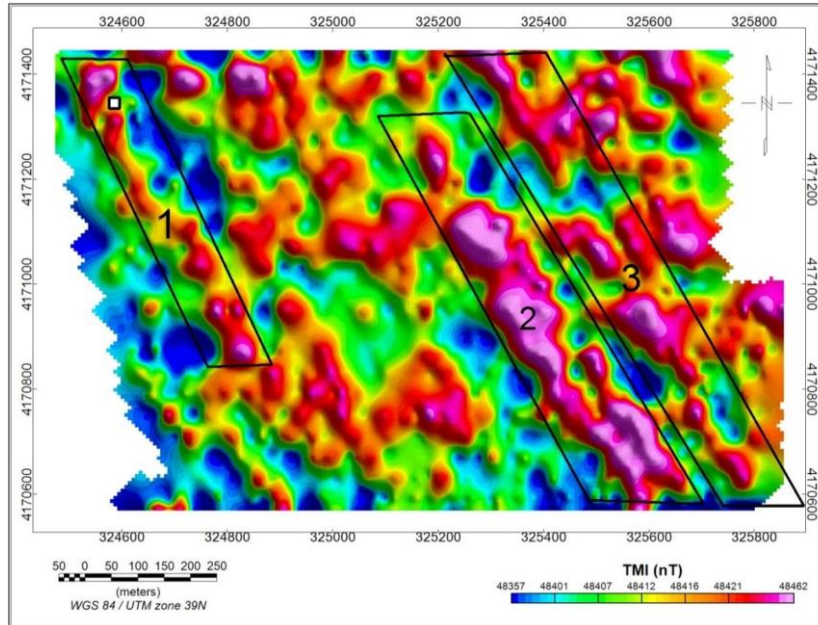


Figure 4: Map of the total magnetic field. The surveying points are drawn with hollow circles. The small white square in the upper left corner is spring location. The three revealed linear trends are shown in the box.

1-4- Using Filter For Recognition of Magnetic Anomalies

For processing and interpretation of the magnetic field maps, and recognition of magnetic lineaments some method is used. Some of these conversions are as follows:

1-4-1- Conversion to Magnetic Pole

In this method by using the magnetic field of the georeferenced, the amount of anomaly related to the interior earth eliminated (Figure 5). In this map, linear trends can be seen more clearly than the total magnetic field map. The anomaly No.4 recognized using this conversion. Trends 1, 2 and 3 are amplified, but trend 3 is more clear in total magnetic field map.

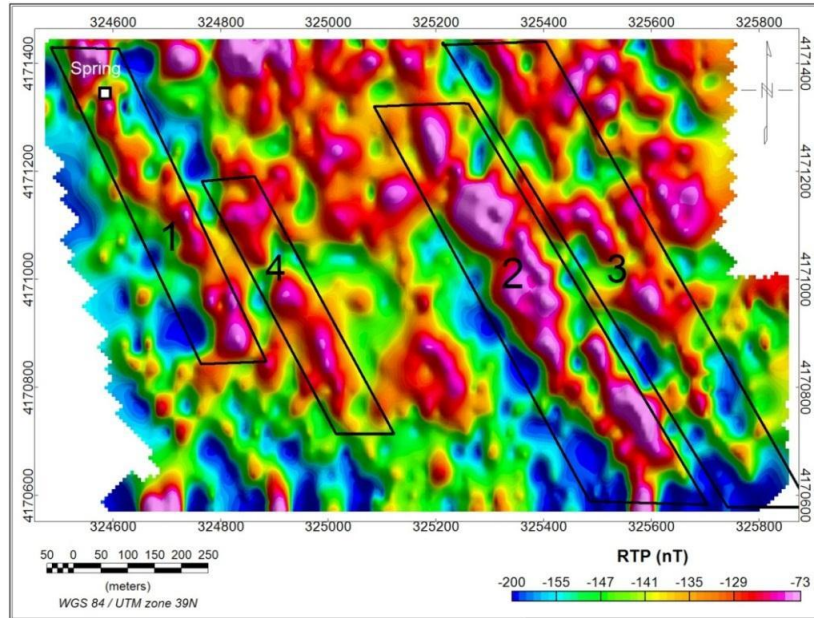


Figure 5: The map of converted magnetic anomaly pole.

1-4-2- Vertical derivative

The trends of the surface magnetic, using this filter are more clear (Figure 6). The linear trends are clear in frames number 2 and 3. In frame 2, there are 2 trend near together in the southern part of Figure 6, which transform to one trend in the upper part. With this filter two more anomalies i.e. frames 5 and 6 are recognized.

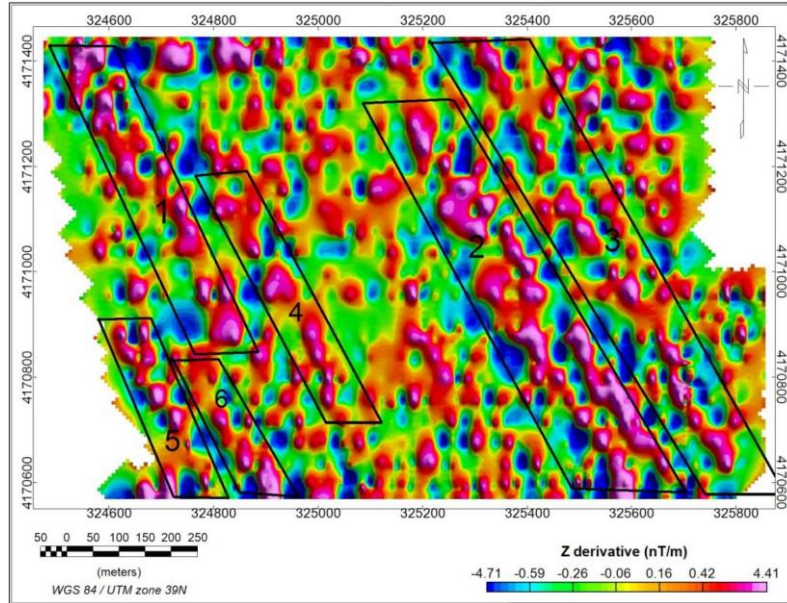


Figure 6: Map of the vertical derivative of the magnetic field on converted magnetic pole. Magnetic linear trends can be observed clearly.

1-4-3- Horizontal Derivative

With this filter, the edge of magnetic sources is clear, and the probable reason, is the high dip of the anomaly sources (Figure 7). In frames 2, 3, 5 and 6 it is possible to recognize the edge of sources, but not for frames 1 and 4. In frames 5 and 6, it can be seen that these two lineaments are continues, and could be related to one geological unit. This is the better method for recognition of magnetic trends in this study.

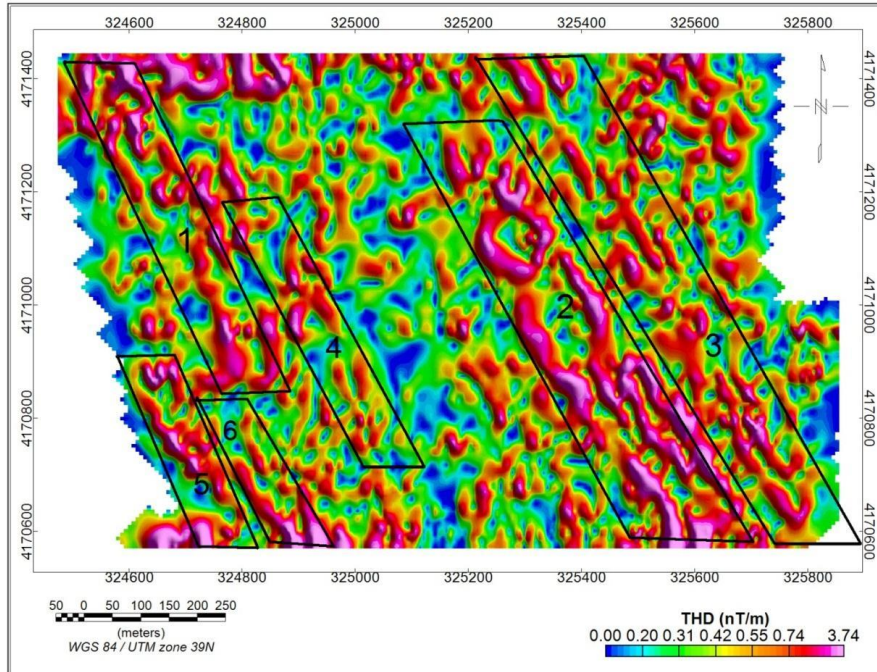


Figure 7: Map of the perfect horizontal derivative of the magnetic field converted to magnetic poles.

1-4-4- Analytical Signal

In Figure 8, the result of analytical signal over the magnetic pole conversion is shown. Except lineaments 2, 5 and 6, the other linear trends are not clear. In this method, like the horizontal derivative, trends 5 and 6 are related to one trend. On the basis of obtained results, the analytic signal, is not a good method for this study.

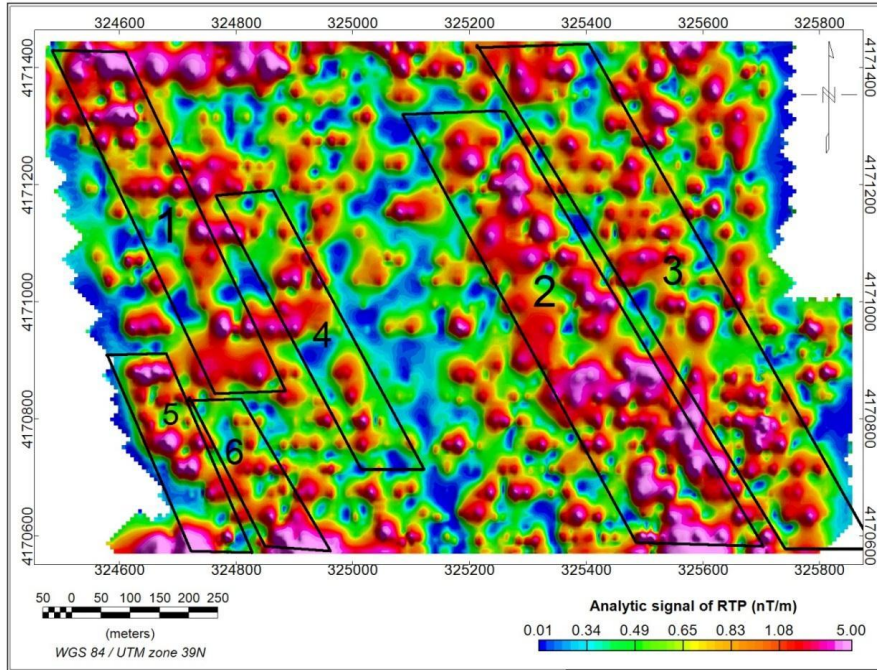


Figure 8: Analytical signal map of magnetic field converted to magnetic pole.

1-4-5- Upward Continuation

This method used to study behavior of the anomaly sources with increasing height, and separation of anomaly sources in different levels. Upward continuation of 10 m, 20 m, 40 m, 60 m, 80 m, 100 m, 120 m and 150 m are shown in Figure 9. With increasing distance, the value of high frequencies and noises will be eliminated.

Geophysical Investigation along the Astara Fault; Geomagnetic and Geoelectric methods

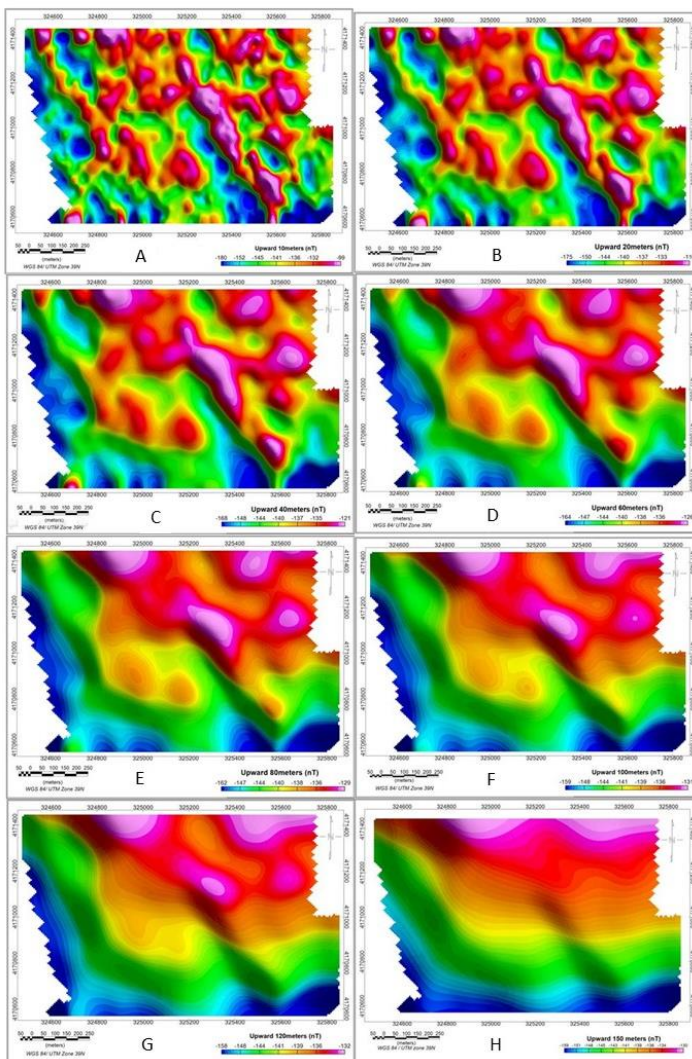


Figure 9: Comparison of the map of conversion to the magnetic pole with the maps of continuing upwards at different altitudes. a) 10 meters. b) Upward continuation to 20 meters. c) 40 meters. d) 60 meters. n) 80 meters. f) 100 meters. e) 120 meters. j) 150 meters. As the height increases, high frequencies are attenuated and deeper anomalies are amplified.

1-5- Gisum Area- Third Stage

In order to better understanding of the position of linear trends, data collection continued to the south of the area. Due to the proximity with Gisum village, it was not possible to survey magnetic method towards the previous grid. In this reason 500 m south of the previous grid, data collection with a new grid and dimension of 300 m × 800 m accomplished. Figure 10, shows the magnetic field anomaly after corrections. Maximum anomaly is -171 Nano tesla, minimum is -94 Nano tesla, and mean value is -143 Nano tesla. In this figure only one linear trend can be seen. For better understanding the position of the lineaments, magnetic field anomalies of two maps are shown in Google Earth image (Figure 11). The trend of linear anomaly in the map of lower part of the Gisum related to the upper map is more E-W.

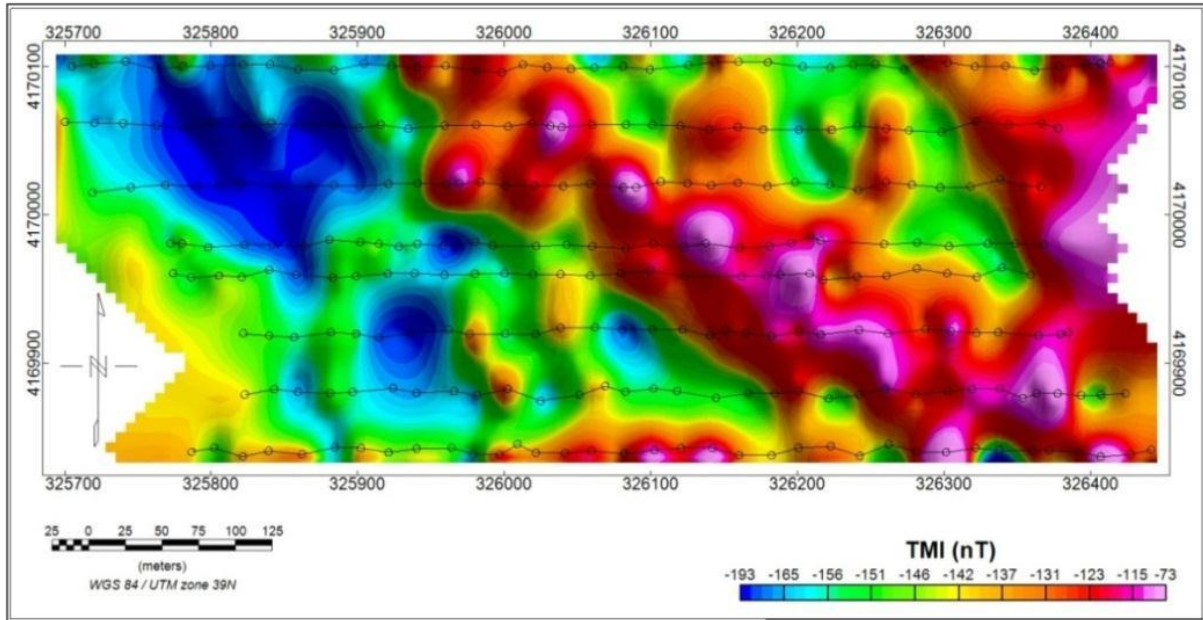


Figure 10: Magnetic field anomaly map after removing the earth's magnetic field component. Surveyed points are marked with hollow circles. The direction of the lines is east-west and is drawn with black lines.

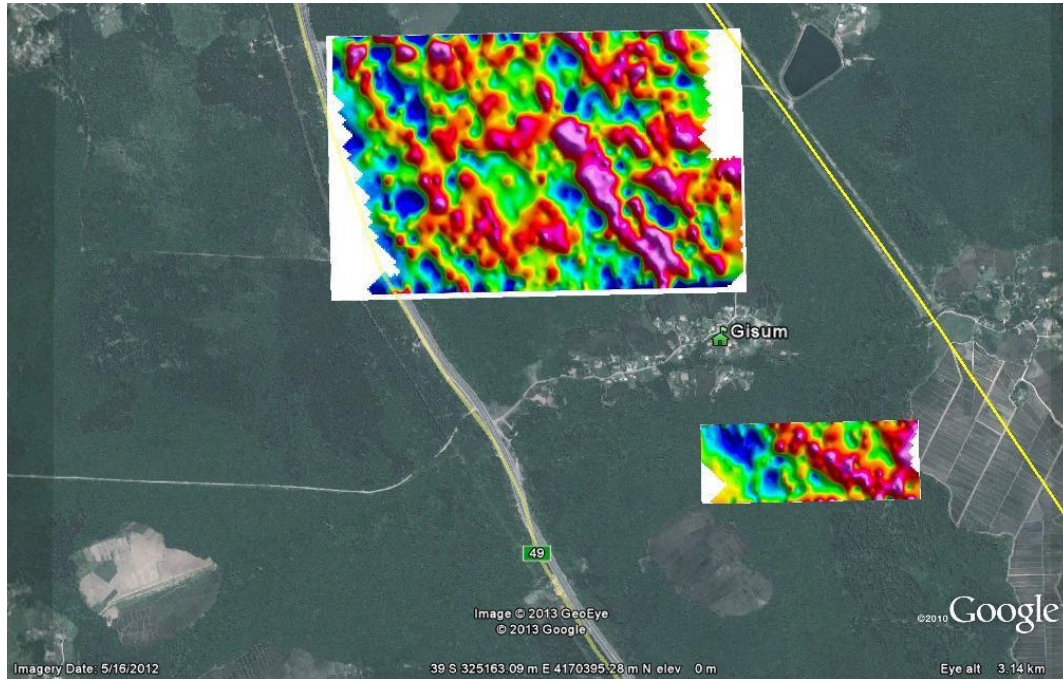


Figure 11: Comparison of magnetic field maps in two arrays in Gisum and location of magnetic linear trends.

1-6- Received Answers for Magnetic Source Depths with Euler Deconvolution Method

In order to understand the depth of the source anomalies, we used the Euler deconvolution method. For a fault with one magnetic contrast and high deep, the ideal value of index structure, is zero. The value of zero to one for a fault with terminated depth and two for faulted thin layers are suitable. While, it is not possible to make a comment for geological structure of a magnetic source, in order to obtain the best result and to determine the source depth and with regards of linear trend of magnetic anomaly, the structure indices and size of different windows examined in the interval 10 to 2.

The results of structural index and different windows are shown in Table 1Table 2Table 3Table 4Table 5.

Table 1: Euler's equation solutions for the window size of 68 meters

Number of answers	standard deviation (m)	Average depth (m)	Maximum depth (m)	Minimum depth (m)	structure index	Euler window (m)	cell size (m)
1030	4.3	15	36	6	0.1	68	6.8
1380	4.7	15	39	6	0.25	68	6.8
1931	5.4	17	44	8	0.5	68	6.8
2426	6.1	19	45	9	0.75	68	6.8
2786	6.8	22	51	9	1	68	6.8
3028	7.5	24	57	10	1.25	68	6.8
3124	8	27	63	10	1.5	68	6.8
3158	9.1	29	69	12	1.75	68	6.8
3142	9.9	32	75	12	2	68	6.8

Table 2: Euler's equation solutions for the window size of 102 meters

Number of answers	standard deviation (m)	Average depth (m)	Maximum depth (m)	Minimum depth (m)	structure index	Euler window (m)	cell size (m)
752	3.3	13	24	7	0.1	102	6.8
1274	3.5	14	27	7	0.25	102	6.8
2706	4	16	31	7	0.5	102	6.8
4089	4.5	18	36	9	0.75	102	6.8
4928	5.1	21	41	10	1	102	6.8
5424	5.8	23	47	10	1.25	102	6.8
5699	6.6	27	52	11	1.5	102	6.8
5834	7.4	30	58	12	1.75	102	6.8
5855	8.2	33	66	13	2	102	6.8

Table 3: Euler's equation solutions for the window size of 136 meters

Number of answers	standard deviation (m)	Average depth (m)	Maximum depth (m)	Minimum depth (m)	structure index	Euler window (m)	cell size (m)
305	2.8	14	22	8	0.1	136	6.8
655	3.3	14	25	8	0.25	136	6.8
1777	3.7	15	30	8	0.5	136	6.8
3393	4.2	17	35	9	0.75	136	6.8
4521	4.7	20	43	11	1	136	6.8
5049	5.3	23	48	13	1.25	136	6.8
5293	6	27	55	14	1.5	136	6.8
5385	6.7	31	60	15	1.75	136	6.8
5437	7.4	34	65	15	2	136	6.8

Table 4: Euler's equation solutions for the window size of 150 meters

Number of answers	standard deviation (m)	Average depth (m)	Maximum depth (m)	Minimum depth (m)	structure index	Euler window (m)	cell size (m)
no answer	no answer	no answer	no answer	no answer	0.1	150	15
1	-	26	26	26	0.25	150	15
4	2	28	31	26	0.5	150	15
27	5.2	27	36	17	0.75	150	15
69	5	29	41	20	1	150	15
193	5.8	30	46	20	1.25	150	15
333	5.7	33	52	24	1.5	150	15
482	6	37	57	26	1.75	150	15
617	6.4	40	63	29	2	150	15

Table 5: Euler's equation solutions for the window size of 210 meters

Number of answers	standard deviation (m)	Average depth (m)	Maximum depth (m)	Minimum depth (m)	structure index	Euler window (m)	cell size (m)
no answer	no answer	no answer	no answer	no answer	0.1	210	15
no answer	no answer	no answer	no answer	no answer	0.25	210	15
no answer	no answer	no answer	no answer	no answer	0.5	210	15
no answer	no answer	no answer	no answer	no answer	0.75	210	15
24	9.1	26	31	23	1	210	15
1439	3.9	25	40	17	1.25	210	15
2111	4.4	28	46	18	1.5	210	15
645	4.1	35	47	26	1.75	210	15

1-7- Resistivity Profiles and Induced Polarization

In order to study the obtained linear magnetic traces and depth of the anomaly sources in Gisum area, we measured eight resistivity profiles and induced polarization perpendicular to linear magnetic trends in three different localities (Figure 12 & Figure 13).

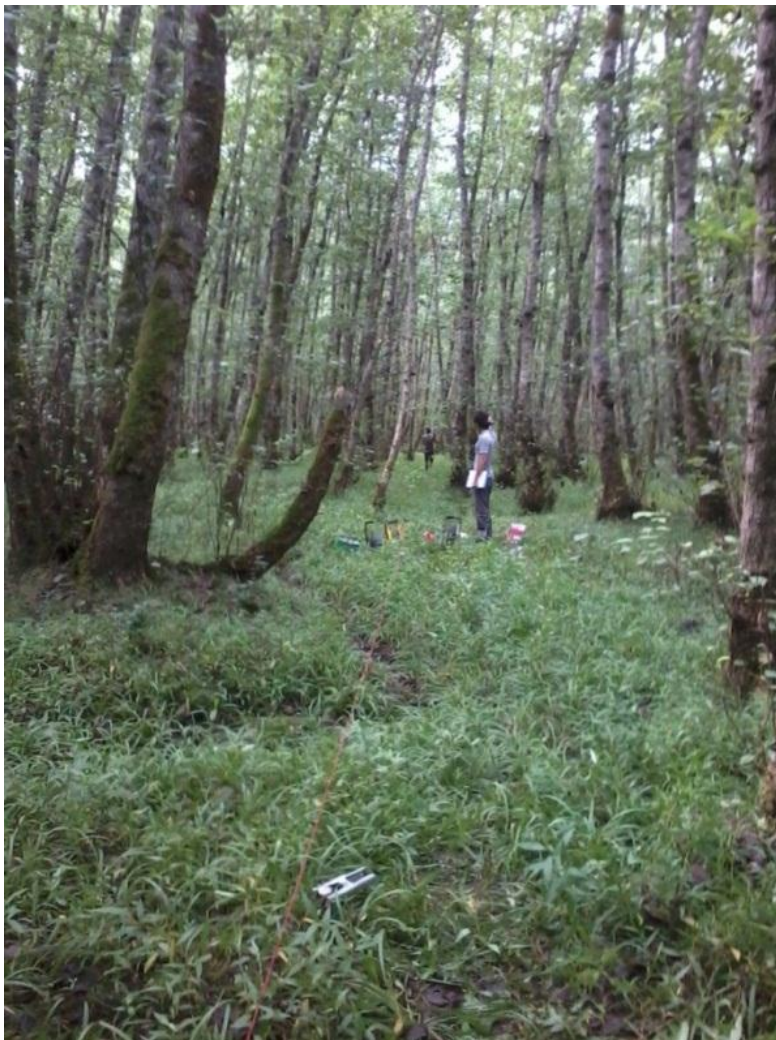


Figure 12: A view of the geoelectric surveying site in Gisum region. View to the southwest.

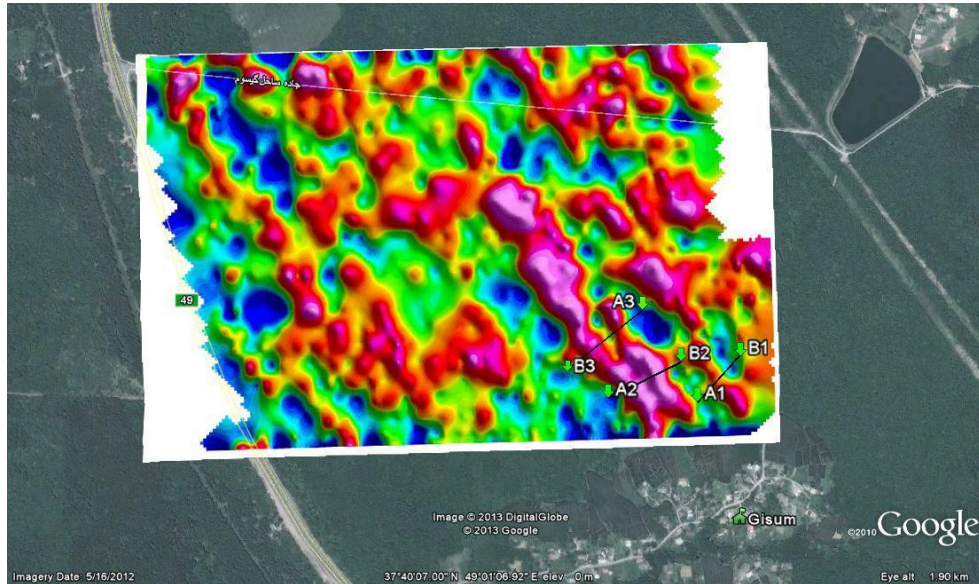


Figure 13: Location of three geoelectric measurements on the magnetic field map and Google Earth satellite image.

The extract of all profiles and pseudosections, are shown in Table 6. and the results of measured pseudosection localities and correlation of their location with linear magnetic trends can be seen in Figure 14Figure 15Figure 16Figure 17Figure 18Figure 19Figure 20.

Table 6: The information about the profiles taken by the methods of induction polarization and resistivity of Gisom is given in this table.

profile	Array type	Profile length (m)	Electrode distance (m)	Checkable depth (m)	Chargeability changes (ms)	Resistivity ($\Omega.m$)
1	dipole-dipole	170	6	12	0.002-10	3-80
2	dipole-dipole	190	10	22	0.1-46	5-98
3	dipole-dipole	170	10	22	-	11-78
4	dipole-dipole	210	15	33	0.01-18	7-102
5	dipole-dipole	220	20	43	-	8-100
6	dipole-dipole	200	12	47	0.00014-3.5	12-274
7	pole-dipole	200	12	47	-	10-110

Geophysical Investigation along the Astara Fault; Geomagnetic and Goelectric methods

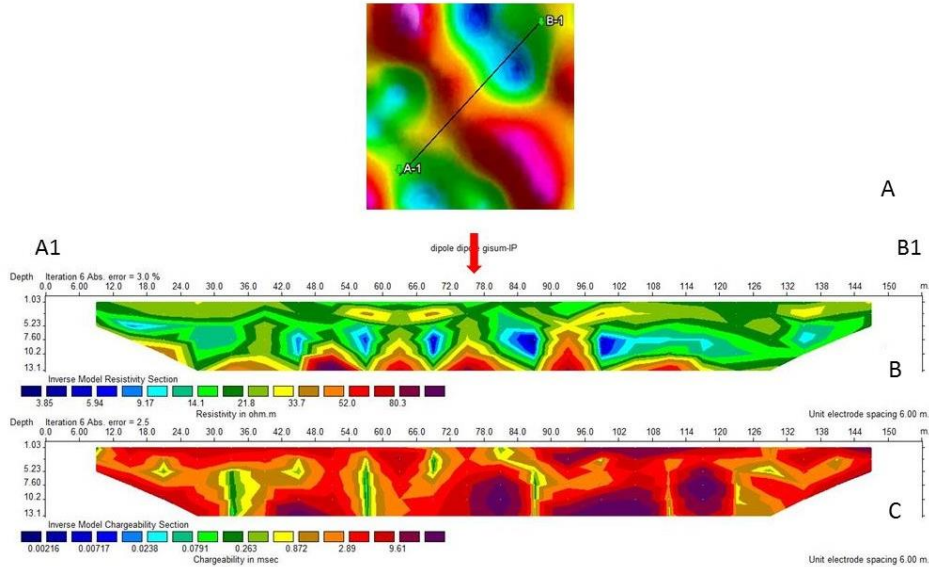


Figure 14: A) The location of surveyed electric profile with the dipole-dipole array on the magnetic field map. b) Electrical resistance quasi-section. c) Chargeability quasi-section. The red arrows on the pseudo-sections indicate the location of the linear anomaly.

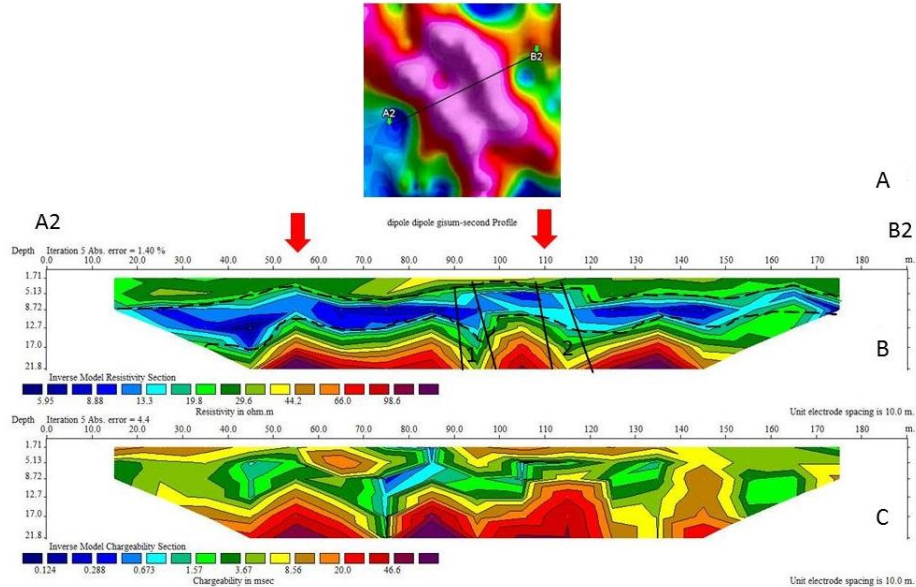


Figure 15: A) The location of measured electric profile with the dipole-dipole array on the magnetic field map. b) Electrical resistance quasi-section. c) Chargeability quasi-section. The area inside the dashed line is the groundwater table. 1 and 2 show areas with lower resistance.

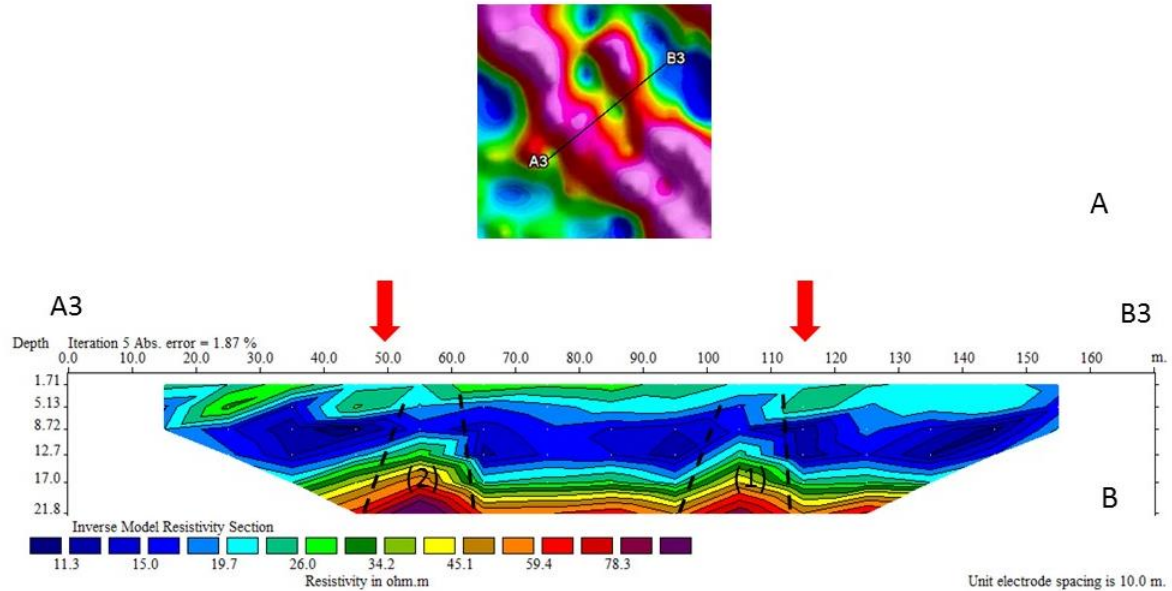


Figure 16: A) The location of measured electric profile with the dipole-dipole array on the magnetic field map. b) Electrical resistance quasi-section. Corresponding to magnetic anomaly, electrical anomaly is observed. 1 and 2 show areas with higher resistance.

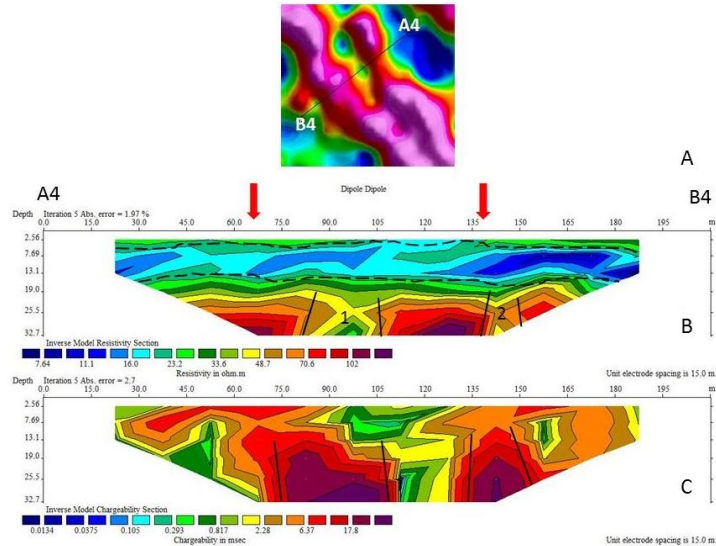


Figure 17: A) The location of surveyed electric profile on the magnetic field map. b) Electrical resistance quasi-section. c) Chargeability quasi-section. Corresponding to the magnetic anomaly, the electrical anomaly is seen in the quasi-sections. The area inside the dashed line is the groundwater numbers. 1 and 2 show areas with lower resistivity.

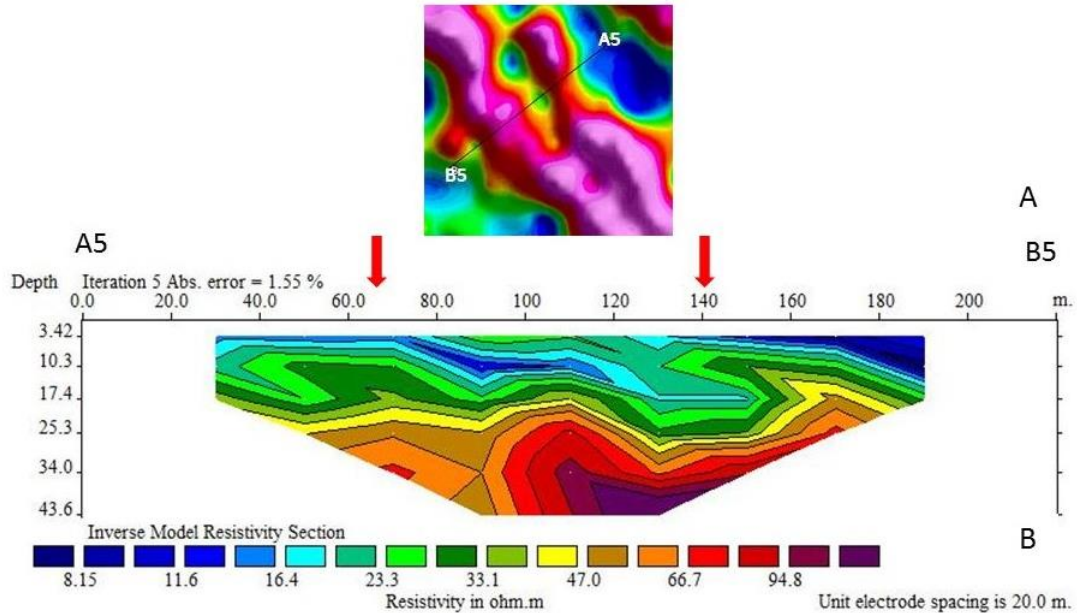


Figure 18: A) The location of surveyed electric profile on the magnetic field map. b) Electrical resistance quasi-section.

Geophysical Investigation along the Astara Fault; Geomagnetic and Geoelectric methods

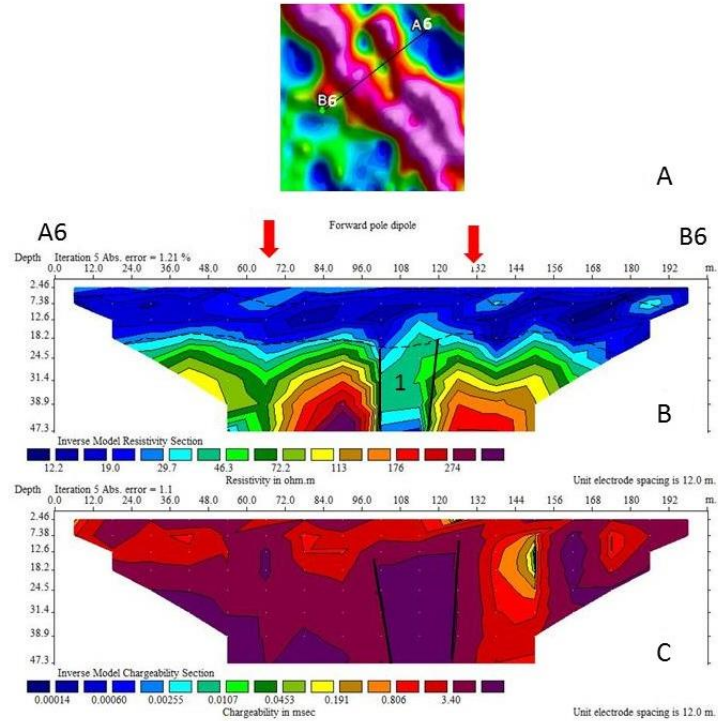


Figure 19: A) The location of surveyed electric profile by the polar-dipole method on the magnetic field map. b) Electrical resistance quasi-section. c) Chargeability quasi-section. Corresponding to the magnetic anomaly, the electrical anomaly is also observed. The area inside the dashed line is the groundwater table. 1 and 2 show areas with lower resistance and higher chargeability.

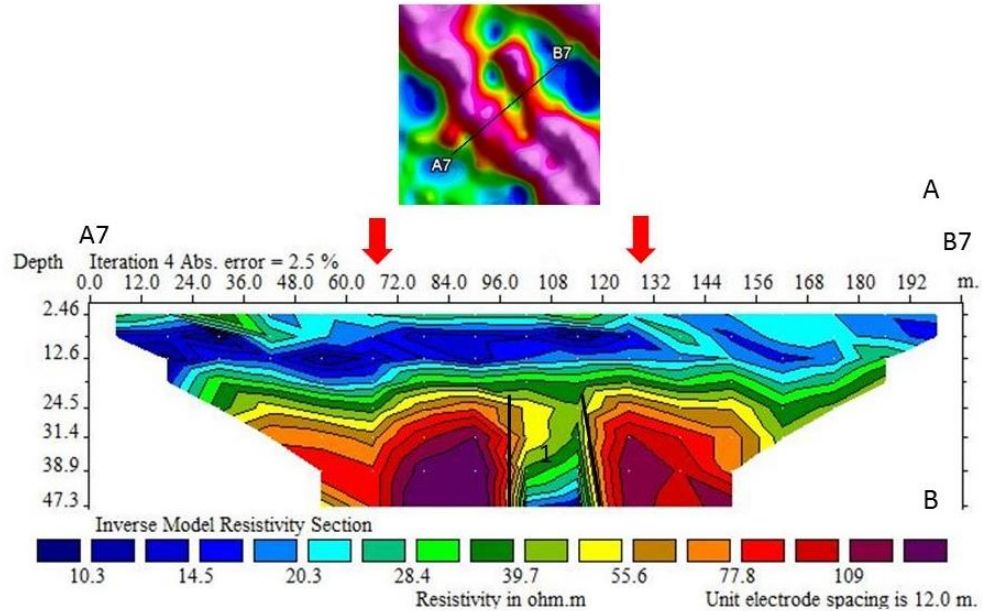


Figure 20: A) The location of surveyed electric profile with the reversed polar-dipole array on the magnetic field map. b) Electrical resistance quasi-section. Number 1 indicates the area with lower resistance.

1-8- Lissar Area

The area under study located 27 km north of Talesh city, near Harehdasht village (Figure 21).

Magnetic anomaly profile, after removing the magnetic field georeferenced is shown in (Figure 22). There are four magnetic anomalies with wavelengths of 300 m to 500 m in this profile. Amplitude of these anomalies are about 100 to 200 Nano tesla. The probable source of anomalies shown in Figure 23. In two localities the river displaced right laterally, which probably is due to the right lateral movement of the fault. The trace of fault, confirmed for one of the mentioned lateral offset, and position of this fault showed by an arrow in the magnetic profile, which is conformable with anomaly number two. In order to confirm that mentioned anomaly is related to faulting, we need two dimensional measurements or geological structures modelling.

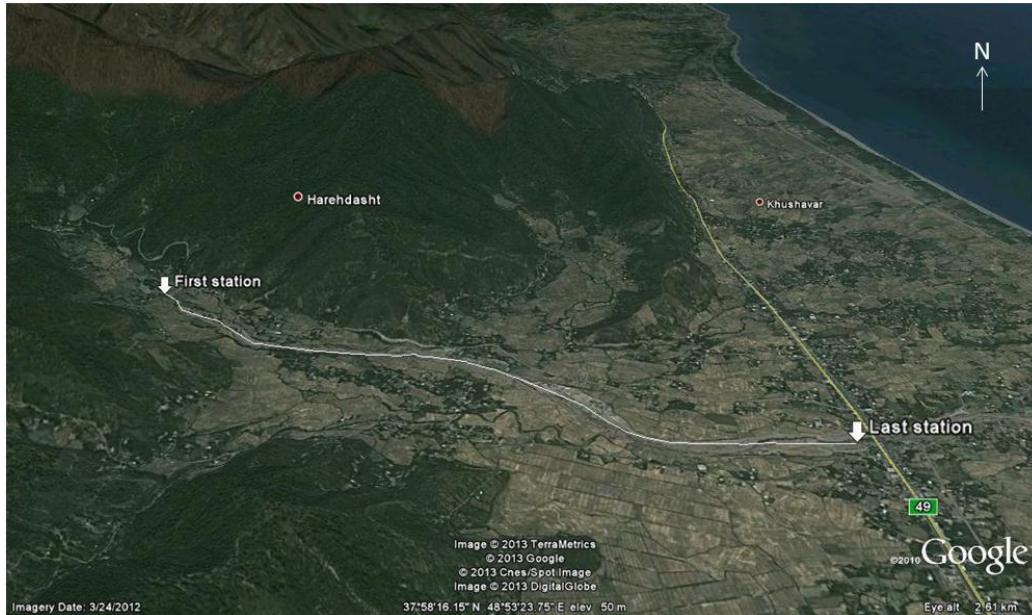


Figure 21: Geographical location of data collection site in Lisar area near Hareh Dasht village. The start and end of the surveying points are marked with white arrows. The white line shows the navigation trend.

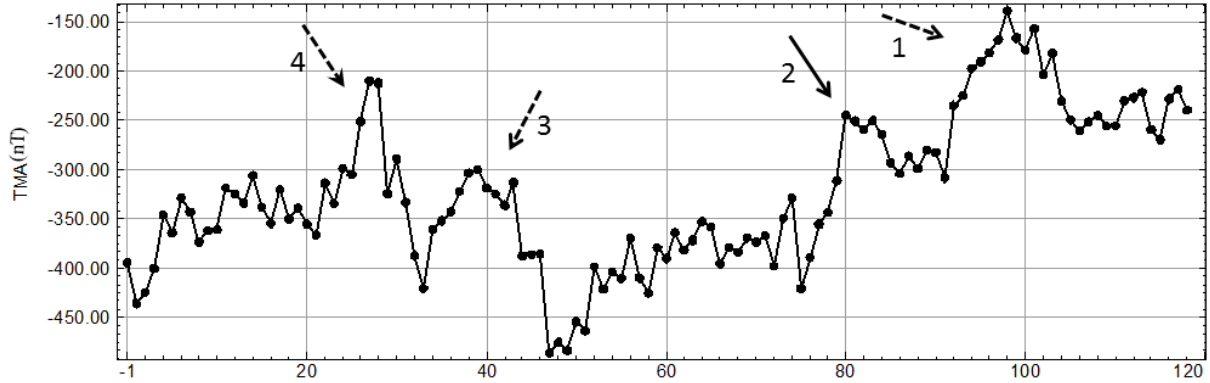


Figure 22: Anomalous profile of the magnetic field carried out along the river in Lisar. The location of the fault introduced by the Geological Survey of Iran is indicated by arrow number 2. The rest of the arrows show the location of the revealed abnormalities.

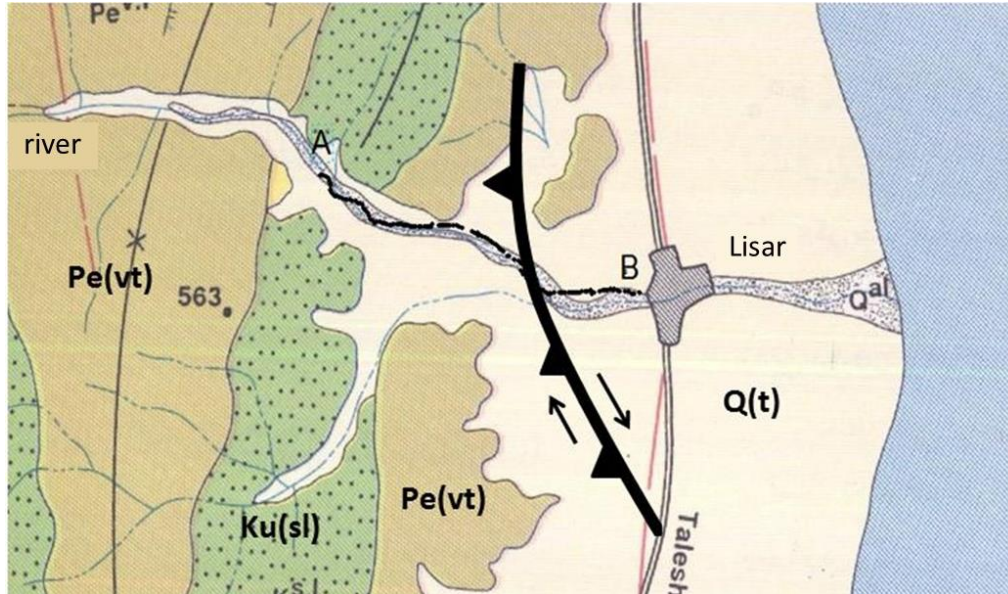
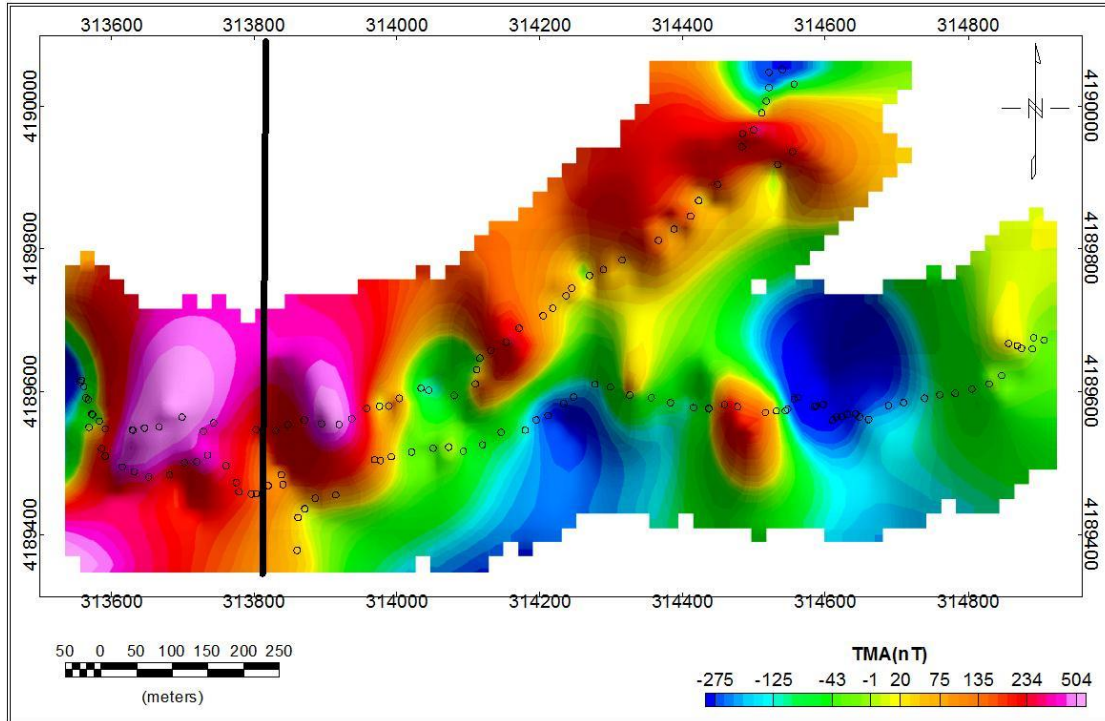


Figure 23: Geological map of the studied area. The surveying points are marked with a circle on the AB line. Q(t): alluvial sediments and alluvial fans. Ku(sl): sandy limestones of Upper Cretaceous age. Pe(vt): andesitic tuffs of Pliocene age. The reverse fault with strike-slip component is marked with a black line.

1-9- Talesh area

This area is located north of Talesh city. The interval of measured points are 30 m and total number of measured points are 136. Figure 24, shows the total magnetic field on the Google Earth image, with location of fault and shutter ridge landform. This shutter ridge with N-S trend, is parallel with fault trend.



Geophysical Investigation along the Astara Fault; Geomagnetic and Goelectric methods

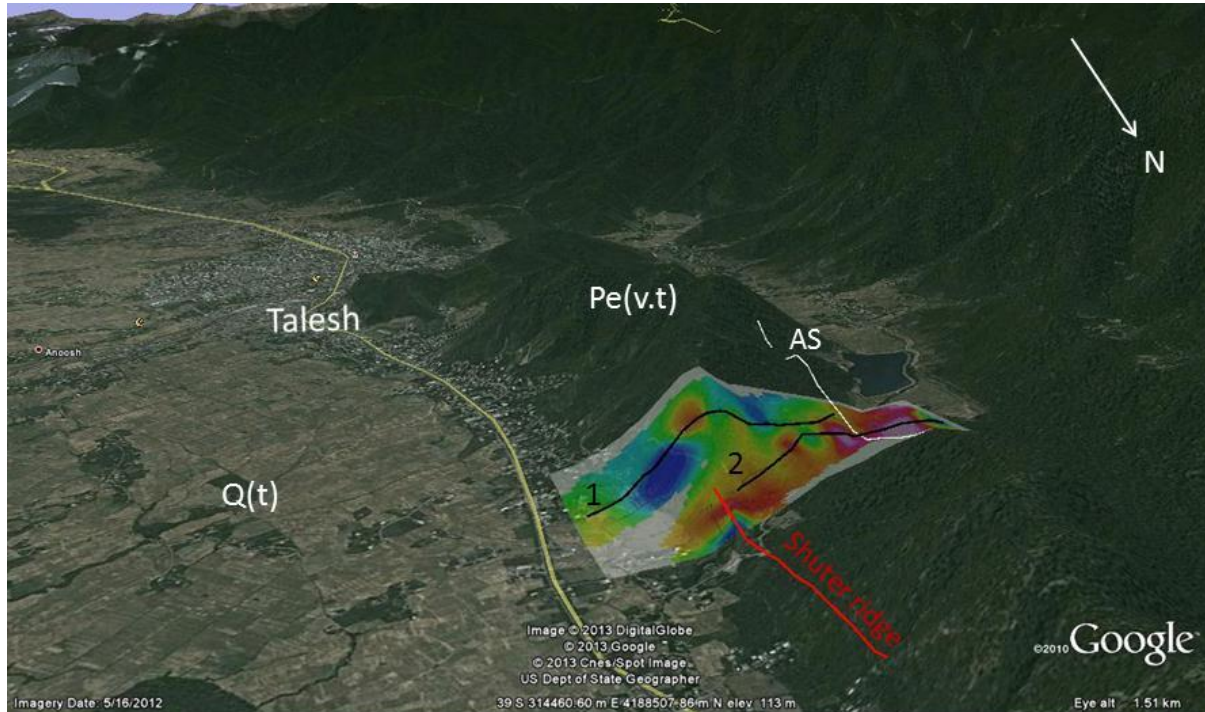


Figure 24: Bottom: Magnetic field anomaly map on Google Earth image. Measured lines in black. The designated fault is marked with a white line and the shutter ridge is marked with a red line. Q(t) Quaternary alluvial sediments and Pe(v.t) is andesitic tuffs. Figure above) Magnetic anomaly map. The black north-south line of the Astara fault has been determined by the Geological Survey of Iran.

1-10- Jokandan Area

This area is located 10 km north of Talesh city. Distance between points are 30 m and total number of measured points are 718. Figure 25 shows the map of anomaly field after removing the magnetic field georeferenced. The minimum field of Nano tesla is -538, maximum is 562 Nano tesla, and mean value is -265 Nano tesla. In the canal course, between points C and D, the amount of anomaly amplitude in the AB magnetic profile is about -550 Nano tesla. The question is why there is such a small amplitude between C and D? In this regard the magnetic field map is overlaid on the geological map of the area (Figure 26). Here it can be seen that the material of two sides of the canal with large magnetic amplitude are volcanic rocks and along the canal course this volcanic rocks, covered by the Quaternary sediment. It is worth to mention that anomalies C and D are located in hills with 100 m height, and can not be observed along the length of the volcanic outcrop.

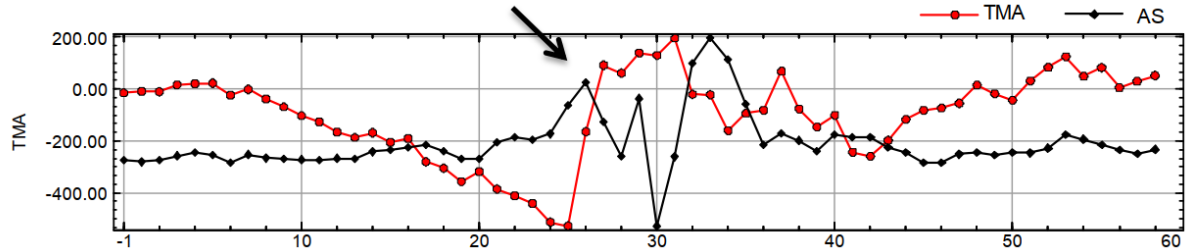
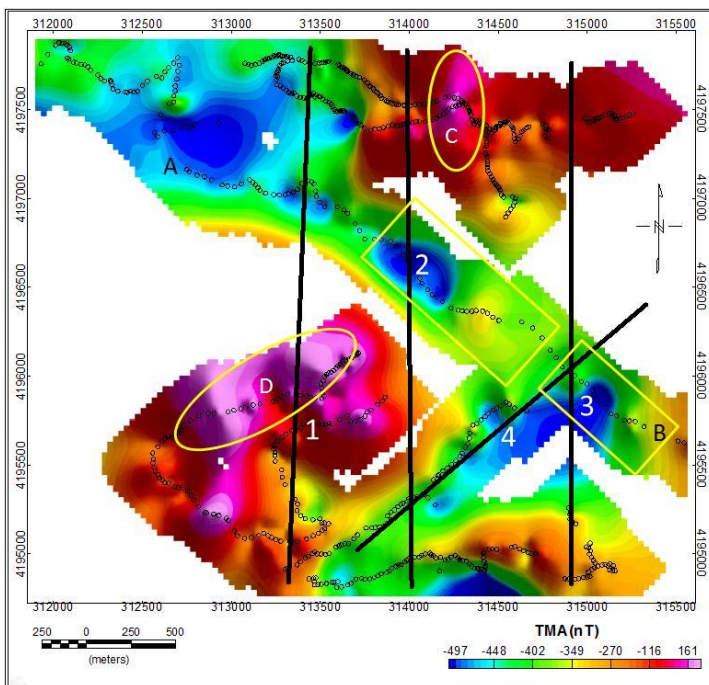


Figure 25: The magnetic anomaly profile (TMA) in Talash is plotted with a red circle and the analytical signal (AS) with a black square. The arrow shows the location of the shutter ridge.

Geophysical Investigation along the Astara Fault; Geomagnetic and Geoelectric methods



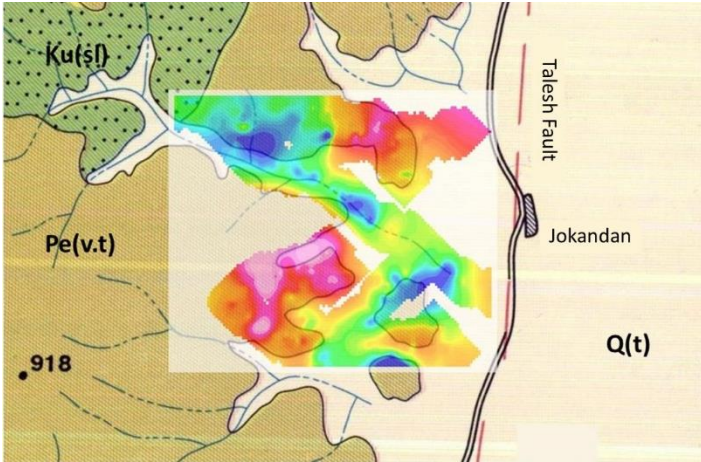


Figure 26: Above) Magnetic field anomaly map in Jokandan region. Surveying points are marked with circles on the map. The black lines numbered 1 to 4 are faults determined by the Geological Survey of Iran. The two yellow boxes are anomalies suspected to be caused by faulting. (bottom figure) magnetic field map on the geological map of the area. Q(t): Quaternary alluvial deposits. Pe(v.t): Pliocene andesitic tuffs. Ku(sl): Upper Cretaceous sandy limestone.

In Figure 26, two anomalies with more or less same amplitude and shape are shown in a yellow color frame. So, for more information a NW-SE profile with 3 km long along the river course carried out (Figure 27). The points with maximum analytical signal that show the boundary of causative sources, are in agreement with fault line.

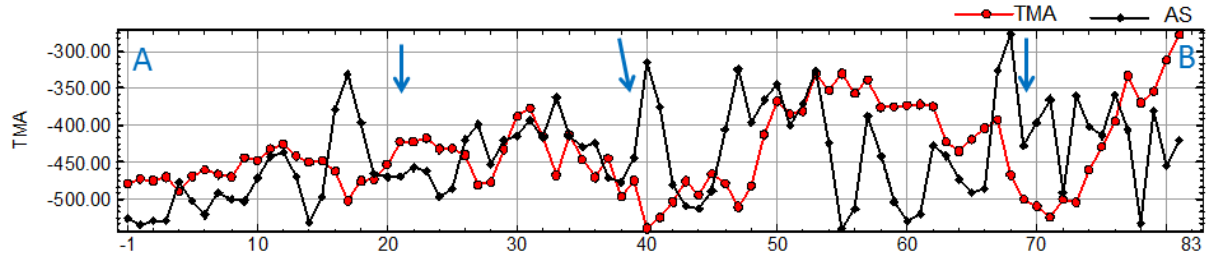


Figure 27: The profile of magnetic anomaly (red color) and analytical signal (black color) of AB in the river course of Jokandan region. The blue arrows are the locations of the faults determined by the Geological Survey of Iran.

2- Discussion and Conclusion

GPS vectors, indicate a right lateral movement along the Astara fault in Talesh region, that is in agreement with morphotectonic evidences. These studies also indicate the fault propagation towards the east.

Due to the lack of previous geophysical investigation, a comprehensive geomagnetic and geoelectric measurement carried out along the fault in different regions.

2-1- Lissar Area

In this region, right-lateral movement of the fault, caused displacement of the river. Surveyed magnetic profile with 4 km. length along the river is indicator of four original magnetic anomalies. Due to the lack of data about the sub-surface geology, it is not possible to talk about the source of these anomalies, but one of them is coincidence with fault trace.

2-2- Talesh Area

Two magnetic anomaly obtained in this area, which one the anomaly is coincidence with the trace of Astara fault, but it is not possible connect it definitely to faulting. There is a considerable magnetic anomaly in the western part of the mountain front. This is coincidence with a N-S trend shutter ridge.

2-3- Jokandan Area

The observed magnetic anomaly with lesser amplitude along the river, might be indicator of alluvial sediment coverage and depth of anomaly sources. With this assumption, it is possible to consider a linear magnetic anomaly, which produced by faulting. To confirm this interpretation, drilling operations and self-existing measurement of rocks are necessary.

2-4- Gisum Area

In order to detect the Astara fault trace, a comprehensive surveying with a length of 7 km performed in Gisum area. In prepared magnetic field map, the trace of major fault was not clear, but in some places, it was possible to observe a weak anomaly. In this reason the second stage of surveying carried out along one of these anomalies.

The vertical and horizontal derivative filters, showed clearly the edges of the anomaly sources, but the result of analytical signal was not acceptable. This might be probably due to the high depth of the anomaly source with respect to it thickness. The acceptable response of magnetic field to vertical and horizontal derivative, and short wave length of observed magnetic linear trends, also indicating the low depth of magnetic sources.

In order to estimates the depth of the major line, the Euler deconvolution method used. With regards to the density of responses, and changing the trend of

obtained depths, the best obtained response for structure index is 0.5 m and for depth are 15 m to 22 m.

Eight resistivity and induced magnetization profiles measured, perpendicular to the linear trends in three different localities. In four profiles, the resistivity anomalies are coincided with magnetic anomalies.

The high resistivity of deeper layers might be due to sand and gravel beds. Penetration of water and clay, increased their chargeability. Overlapping of the electric resistivity of clays is a major problem for interpreting results of electric resistivity. The electric resistivity of clay is 1 to 100 and water 10 to 100 ohm.m., which start from the surface and continued to the depth of 15 – 20 m.

On the whole, depth of anomaly sources obtained from pseudosections, are 18 m to 25 m, which more or less are equal to depths obtained from the Euler deconvolution.

2-4-1- Are Detected Linear Structures are Indication of Buried Faulting

In order to detect the Astara fault trace, a comprehensive surveying performed along the fault. The aim of this study is determine whether or not the linearity of trend related to faulting. The linearity of trends probably proved the strike-slip sense of movements along the fault. It must be noticed that the depth of anomalies, is not the depth of source, and it is

possible that fault plane is shallower than the measured amount. Filters used for magnetic field showing shallower depth with low thickness of sources. Pseudosection of electric resistivity and chargeability also, indicating a shallower depth and high dip of sources.

In conclusion, the source of anomalies is shallow with steep dip (more or less vertical) and low thickness. The obtained shallow depth of sources, more or less vertical with low thickness may indicator of faulting in depth, which is not reached to the ground surface yet. However, interpreted magnetic anomalies in Jokandan, Lisar and Talesh are in agreement with morphological indices such as offset streams and shutter ridges.

References

Milsom J., 2003. Field geophysics, Wiley-Blackwell, 3rd Edition, 244.

Reeves, C., 2005. Aeromagnetic surveys. Geosoft.